Cell Calcium (2002) **32**(4), 217–229
0143-4160/02/$ – see front matter
doi:10.1016/S0143-4160(02)00157-4, available online at http://www.idealibrary.com on IDEAL®

On the conservation of fast calcium wave speeds

L. F. Jaffe

The OB/GYN Department, Brown University, Providence, RI, USA

Summary Calcium waves were first seen about 25 years ago as the giant, 10 μm/s wave or tsunami which crosses the cytoplasm of an activating medaka fish egg [J Cell Biol 76 (1978) 448]. By 1991, reports of such waves with ∼10 μm/s velocities through diverse, activating eggs and with ∼30 μm/s velocities through diverse, fully active systems had been compiled to form a class of what are now called fast calcium waves [Proc Natl Acad Sci USA 88 (1991) 9883; Bioessays 21 (1999) 657].

This compilation is now updated to include organisms from algae and sponges up to blowflies, squid and men and organizational levels from mammalian brains and hearts as well as chick embryos down to muscle, nerve, epithelial, blood and cancer cells and even cell-free extracts. Plots of these data confirm the narrow, 2–3-fold ranges of fast wave speeds through activating eggs and 3–4-fold ones through fully active systems at a given temperature. This also indicate Q_{10}'s of 2.7-fold per 10 °C for both activating eggs and for fully activated cells.

Speeds through some ultraflat preparations which are a few-fold above the conserved range are attributed to stretch propagated calcium entry (SPCE) rather than calcium-induced calcium release (CICR).

Table 1a provides an updated list of waves through fertilizing eggs from a fucoid alga up to mice; while Table 1b provides such a list for calcium waves through fully active systems from droplets of cytoplasm of the common pond alga, Chara (case #73) up to the human brain (cases #26–26b). The corresponding Fig. 1A–C plot speed versus temperature through activating eggs, through other individual but fully active cells and across tissues (or other groups of cells), respectively. As was shown long ago [2] the speeds of fast calcium waves through activating eggs–here shown in Fig. 1A–are a few-fold below those through those through full active systems as shown here in Fig. 1B. This speed depression may be attributed to the dearth of various ER calcium release channel modulators (cyclic AMP, IP3, NADP, etc.) in highly repressed oocytes or eggs before activation. However, mean speeds through tissues–shown in Fig. 1C–are *not* clearly below those in fully active cells as shown in Fig. 1B. While these collective data fail to reflect intercellular or cell–cell delays, some observation on individual systems, do. Thus, intercellular calcium wave speeds through blowfly salivary glands (case #49) are about 40% below intracellular ones in this tissue (case #49a); while the transtissue speed through rabbit airway cell monolayers (case #59) are likewise about 40% below the intracellular one. Perhaps, evolution minimizes the cell–cell delays of calcium signals through tissues.

For both activating eggs and for waves through fully active cells, the collective wave speed rises about 2.7-fold per 10 °C rise in temperature; while the collective Q_{10} for tissues etc. seems to be about 3.0-fold, and thus, a bit higher. Moreover, speed versus temperature data are available for three individual systems. Such data for waves of spreading depression through the cerebellum of the skate are plotted in Fig. 1C and show a Q_{10} which is indistinguishable from the collective one. The same is true for data obtained from observations of contraction waves through isolated rat heart muscles as plotted in Fig. 1B. However, the remarkable velocity versus temperature data for calcium waves through isolated human uterine myocytes (case #17a [66]) seems to show a somewhat lower Q_{10}.

Among the more interesting new speed data since the 1991 compilation [2] is a very old one through an activating fucoid egg (case #1 in Table 1a [5]) and quite recent

Received 16 May 2002
Revised 29 July 2002
Accepted 29 July 2002

Correspondence to: Dr Lionel F. Jaffe, Marine Biological Laboratory, 7 MBL Street, Woods Hole, MA 02543, USA. Tel.: +1-508-289-7251; fax: +1-508-540-6902; e-mail: ljaffe@mbl.edu

Table 1a A list of fertilization waves with known speeds

Case	Group	Genus	μm/s at °C	Indicator	Reference
1[a]	Fucoid algae	*Cystoseira*	5 at 18	Secretion	[5]
2	Sponges	*Tetilla*	9 at 19	Secretion	[6]
3[b]	Crustacea	Marine shrimp	20 at 22	Fluo-3	[7]
5	Echinoderms	*Arbacia*	12 at 26	Secretion	[8]
6		*Comanthus*	6 at 24	Secretion	[9]
7		*Psammechinus*	8 at 18	Secretion	[10]
8		*S. drobechiansis*	3 at 8	Secretion	[11]
9		*S. purpuratus*	6 at 16	Secretion	[12]
10		*Asterias*	6 at 18	Aequorin	[13]
11		*Arbacia*	14 at 19	Aequorin	[14]
12		*Scaphechinus*	10 at 23	Aequorin	[15]
13		*Lytechinus*	8 at 16	Aequorin	[16]
14		*Lytechinus*	11 at 18	Fura-2	[17]
16		*Clypeaster*	16 at 25	Fluo-3	[18]
17		*Pisaster*	6 at 14	Calcium green	[19]
18	Tunicates	*Phallusia*	13 at 20	Aequorin	[20]
18a		*Ciona*	10 at 25	Fura-2	[21]
18b		*Ciona*	11 at 20	Ca green dextran	[22]
19	Hemichordates	*Sacoglossus*	8 at 23	Secretion	[23]
20	Lamprey fish	*Lampetra*	6 at 18	Secretion	[24]
21	Bony fish	*Perca*	7 at 17	Secretion	[25]
22		*Gasterosteus*	8 at 20	Secretion	[26]
25		*Pungitius*	9 at 18	Secretion	[27]
26		Medaka	13 at 26	Aequorin	[1]
26a		Medaka	~12 at 26	Aequorin	[28]
27	Frogs	*Rana*	20 at 22	Secretion	[29]
28		*Xenopus*	8 at 22	Aequorin	[30]
29			10 at 22	Electrodes	[31]
30			8 at 24	Calcium green	[32]
30a			8 at 20	Calcium green	[33]
31			9 at 22	Indo-1 dextran	[34]
32	Rodents	Hamster	22 at 31	Aequorin	[35]
33		Mouse	31 at 32	Green-1 dextran	[36]

[a] This value was obtained from Knapp's estimate that it takes an observed wave of surface roughness about a minute to cross the egg from the observed point of sperm fusion together with a 200 μm figure for the diameter of the egg of *Cystoseira barbata*.
[b] This unusual egg is naturally activated by the increase of Mg^{2+} when it is shed into the sea rather than by sperm attachment which occurs soon thereafter.

ones for brain injury waves obtained via magnetic resonance imaging (MRI, cases #26a–28 in Table 1b [79–83]) and for a cell-free extract made from pig skeletal muscle (case #73 in Table 1b [139]). While most of the speeds are for waves propagated across cells, three (cases #48, 48a, and 73) are centripetal. Moreover, there is a hint of such an inwards wave during fertilization in the nemertian worm, *Cerebratulus* [19]; while Stephano and Gould have claimed that the egg of the echiuroid worm, *Urechis* is activated by a *waveless* calcium pulse. However, their observations could be explained as reflecting an inward activation wave since protostome eggs like those of *Urechis* and *Cerebratulus* do seem to be activated in this way [141].

With some exceptions discussed below (and with due regard for experimental error) the accumulated speed data continue to remain within a 2–3-fold range for ones through activating eggs at a given temperature and a 3–4-fold one for fully active systems, likewise at a given temperature. The narrowness of these ranges may be best appreciated when one considers the nearly billion-fold range of the four main classes of calcium waves as shown in Fig. 2.

These exceptions are in the data points marked by triangles (▲), in Fig. 1B and lie at speeds which are 2–3-fold above the generally conserved range. Most of these are listed under *ventriculocytes* which, in turn, are listed under adult muscle in Table 1b. These are artificial cells created by dissociating the ventricles of adult rodent hearts. Most (but not necessarily all) of them are likely to come from the relatively massive working muscles of the heart rather than its specialized conductive tissues. Importantly, they are only a few microns high (if the order of 10-μm wide and 100-μm long) *and* riddled with invaginating t-tubules so that most of their cytoplasm lies within a micron of the plasmalemma. Furthermore, they exhibit all of the well known phenomena of waves propagated through excitable living systems (such as origin anywhere and self-annihilation when two meet) plus the strange–and perhaps revealing–phenomenon of helical waves [142,143].

Table 1b A list of fast calcium waves through fully active systems

Type	#	Group and system	μm/s at °C	Indicator	Reference
From oogenesis through pattern formation					
C	1	Amphibia, *Xenopus* stage 5 oocyte	25 at 19	Fluo-3	[37]
C	1a		25 at 24	Calcium green	[38]
C	1b		21 at room temperature		[39]
				Ca green dextran	[41]
				Calcium green	[40]
C	2	Annelids, *Chaetopterus* zygote	30 at room temperature	Aequorin	[42]
C	3	Nemerteans, *Cerebratulus* zygote	24 at 14	Dextranned fluorescents	[19]
		From author's Fig. 11g			
C	4	Tunicates, *Phallusia* zygote	25 at 20	Aequorin	[20]
C	4a	*Ciona*	24 at room temperature	Ca green dextran	[43]
C	5	Rodents, hamster zygote	50 at 31	Aequorin	[35]
C	5a	Mouse zygote	20 at 32	Fluorescents	[36]
C	6	Human, sperm injected egg	>51 at 37	Fluo-3 AM	[44]
T	7	Birds, chick streak stage	33 at 37	Contraction	[45]
T	7a		40 at 38		[46]
T	8	Fish, medaka shield stage	33 at room temperature	Contraction	[47]
Adult muscle (all of this muscle data is intracellular)					
C	9	Crustacea, crayfish skeletal	23 at ~20	Contraction	[48]
	10	Frog, whole skeletal	34 at 25	Fluo-3 AM	[49]
	11	Rodents, whole heart	80 at 37	Fluo-3 AM	[50]
	12	Heart muscle	33 at 23	Contraction	[51]
			74 at 30		
	12a	Heart muscle	30 at 33	Fluo-3	[52]
	13	Venous muscle	20 at 25	Fluo AM	[53]
	14	Vascular muscle cell line	16 at 19	Fura-2	[54]
		Ventriculocytes with wave speeds in the conserved range			
	15	Rat, loosely attached	91 at 37	Contraction	[55]
	15a	Loosely attached	113 at 33	Contraction	[51]
	15b	Loosely attached[a]	~100 at 37	Fura-2 AM	[56]
	15c	Slippery support	~50 at 36	Fura-2 AM	[57]
	15d	Slippery support [57a]	103 at 37	Fluo-3 AM	[58]
	15dd	Wave precedes contraction[b]	76 at ~28	Fura-2 AM	[60]
	16	Guinea pig; non-contracting	32 at 22	Fluo-3	[59]
		Ventriculocytes with anomalously high wave speeds			
	15e	Rat, loosely attached	75 at 23	Contraction	[56]
	15f	Tightly attached via Fig. 2 of [60]	116 at ~28	Fura-2 AM	[60]
	15g	Tight(?) since serum free	~100 at 21	Fluo-3	[61]
	15h	Tight(?) since serum free	76 at 21	Fluo-3 AM	[62]
	15l	Tight(?) since serum free	111 at 25	Fluo-3 AM	[64]
	16b	Guinea pig (high $[K^+]_o$), tight(?) since serum free	60 at 23	Fluo-3 AM	[63]
	17	Human uterine myocyte	18 at 23	Ca green 1-AM	[65]
This value is for the so-called near wave speed within 100 μm of the initiating touch stimulus					
	17a	Human uterine myocyte	10 at 19	Ca green 1-AM	[66]
			16 at 25		
			20 at 30		
			41 at 37		
	18	Mouse, cell line myotubes	35 at 24	Fluo AM	[67]
	19	Chick, leg myocytes	70 at 24		
	20	Rabbit, colon myocyte	23 at 25	Fura-2 AM	[68]
Neural systems: glial networks in healthy retinas (all are tissue data)					
T	21	Turtle near hatching retina	40 at 27	Model	[69]
	22	Chick, day 11 retina	130 at 35	Calcium green	[70]
	23	Mouse, day 17 retina	125 at 30	Fura-2 AM	[71]
	24	Ferret newborn retina	~110 at 35	Voltage	[72]
	24b	Ferret newborn retina	~110 at 31–34	Fura-2 AM	[73]
	24c	Ferret newborn retina	~160 at 31–34	Fura-2 AM	[74]
	25	Rat adult retina	23 at 24	Calcium green AM	[75]
	25a	Rat adult retina	18 at 21	Ca green-AM	[76]
	25b	Rat adult retina	28 at 24	Fluo-4 AM	[77]

Table 1b (*Continued*)

Type	#	Group and system	μm/s at °C	Indicator	Reference
Neural systems: spreading depression or spreading convulsion in the brain					
T	26	Human migraine aura	50 at 37	Scotoma	[78]
	26a	Human migraine aura	68 at 37	MRI	[79]
	26b	Human migraine aura	58 at 37	MRI	[80]
	27	Rat brain's cortex	57 at 37	MRI	[81]
	27a	Rat brain's cortex	70 at 37	MRI	[82]
	28	Whole cat's neocortex	58 at 37	MRI	[83]
	29	Rat neocortical slice	34 at 33.5	Intrinsic optical	[84]
	30	Rat hippocampal organ culture	67 at 36	Fluo-3 AM	[85]
	30a	Rat hippocampal slice	25 at 33.5	Intrinsic optical	[84]
The temperature may have been significantly lower than 33 in the reflectance images since enough time for the deeper parts of the slice to warm up from 20 to 23 room temperature may not have been allowed					
	30c	Rat hippocampal slice	15 at 34.5	Voltage	[86]
	31	Squid *Loligo* retina	39 at 20	Voltage	[87]
	32	Squid *Sepia* retina	30 at 20	Voltage	
	33	Frog retina	17 at 23	Scattered light	[88]
	34	Chick retina	62 at 30	Scattered light	[89]
This may be the most accurate single value for the speed of spreading depression in the literature since it was got in entrapped waves, i.e. by inducing circling depression in rings of isolated retinas which continued for about 30 revolutions at a constant speed					
	34a	Chick retina	63 at 33	Scattered light	[90]
	35	Catfish cerebellum	17 at 25	Voltage	[91]
	36	Cat cerebellum	150 at 38	Voltage	
	37	Skate's cerebellum	8 at 10 13 at 15 18 at 18	Voltage	[92]
	38	Rat's cerebellum	153 at 38	Voltage	[93]
	39	Intact young rabbit's cerebrum	59 at 37	Voltage	[94]
In 3–4-week-old rabbits, the same speed is measured in cases of spreading convulsion as in ones of spreading depression					
	39a	Intact rabbit's cerebrum	50 at 33	Impedance tomography	[95]
	40	Intact rat's neocortex	110 at 37	Voltage	[96]
	40a	Intact rat's neocortex	47 at 38	Laser-Doppler	[97]
	41	Intact rat's hippocampus	100 at 37	Voltage	[98]
	42	Cavy's olfactory cortex	60 at 30	Reflectance	[99]
From my measurements on control images shown in Fig. 2 (65 μm/s) of this paper and in Fig. 13 of [99a] (55 μm/s)					
Neural systems: various intracellular waves					
C	43	Rat hippocampal slice intraglial	15 at 21	Fluo-3 AM	[100]
	44	Rat hippocampal glial culture	19 at room temperature	Fluo-3 AM	[101]
	44a	Rat hippocampal glial culture	22 at room temperature	Fluo-3 AM	[102]
	45	Rat brain astrocyte culture	13 at 22		[103]
	46	Rat PC-12 neuroblastoma cells			
		To soma	84 at 21	Fluo-3 AM	[104]
		To neurite	33 at 21		
	47	Mouse N1E-115 neuroblastoma cells	43 at 29	Fura-2 dextran	[105]
	47a	Mouse N1E-115 neuroblastoma cells			
		To soma	39 at 37	Fura-2 AM	[106]
		To neurite	148 at 37		
Ci	48	Frog isolated ganglion cells	47 at 22	Indo-1 AM	[107]
This is an inwards wave in the core region. The small shift above the generally conserved level is attributable to geometry of inward propagation					
Ci	48a	Rabbit isolated otic neurons	~25 at 31–37	Fura-2 AM	[108]
Epithelia: ectodermal					
T	49	Blowfly salivary intercellular	15 at 23	Fura-2 AM	[109]
C	49a	Blowfly salivary intracellular	27 at 23	Fluo-4 AM	[110]
C	50	Goldfish keratocytes	~66 at 22	Indo-1 AM, 2-photon	[111]
Waves were induced by voltage pulses across isolated, adherent cells and observed in a plane within a micron of the supporting surface					
C	51	Rabbit iris ciliary epithelia: from apex to base	23 at room temperature	Fluo-3 AM	[112]
	52	Mouse lacrimal cell couplets	25 at 26	Fluo-3	[113]
T	53	Sheep lens cell monolayer	33 at 22	Fura-2 AM	[114]

Table 1b (*Continued*)

Type	#	Group and system	μm/s at °C	Indicator	Reference
Epithelia: endodermal					
C	54	Skate hepatocyte clusters	35 at 22	Rhod 2/AM	[115]
T	55	Rat liver tissue	~80 at 37	Rhod 2/AM	[116]
T	55a	Rat liver tissue	40 at 30	Fluo-3 AM	[117]
At 1 nm vasopressin, the lowest concentration which largely avoids intercellular delays					
C	55b	Rat liver hepatocyte group	~40 at 37	Fluo-3 AM	[118]
C	55c	Rat hepatocyte's nucleus	49 at 37	Rhod 2/AM	[119]
Stimulated by 0.5 mM Ach (Fig. 3B) or 1 mM ATP (Fig. 3C)					
C	56	Rat pancreatic acini	58 at 37	Fluo-3 AM	[120]
With minimal stimuli of 0.1 M Ach or 0.5 nM CCK					
C	57	Mouse acinar cell clusters	20 at 26	Fura-2 AM	[121]
Stimulated by 0.5 mM Ach (Fig. 2C) or 200 pM CCK (Fig. 2D)					
C	57a	Mouse acinar cell clusters	25 at 22	Fluo-3 AM	[122]
Speed along the surface					
C	57b	Mouse acinar cell clusters	27 at 25	Fluo AM	[123]
Speed along the surface					
This value was obtained with Ach induced waves and is well within the conserved speed range; however, 13 μm/s was observed with bombesin-induced waves. This value is somewhat below the conserved speed range					
T	58	Rat lung cell monolayer	13 at room temperature	Fura-2 AM	[124]
T	59	Rabbit airway cell monolayer	23 at 23	Fura-2 AM	[125]
My estimate from authors' Fig. 3. The transtissue speed was about 60% of the transcellular one					
	60	Cavy gastric parietal	~30 at 37		[126]
Epithelia: mesodermal					
C	61	Human endothelial cells	50 at 37	Fura-2 AM	[127]
T	62	Bovine endothelial cells	28 at 37	Fura-2 AM	[128]
C	62a	Bovine endothelial cells	30 at 23	Indo-1 AM	[129]
Other systems					
C	63	Rat mast cells	35 at room temperature	Fluo-3 AM	[130]
T	64	Rat leukemic mast cell layer	8 at 25	Fura-2 AM	[131]
C	65	Frog melanotropes' cytoplasm	33 at 20	AM fluorescents	[132]
C	65a	Nucleus	80 at 20		
Ci	65b		40 at 20	Fura-red AM	[133]
These are repetitive, spontaneous waves in isolated, flattened cells. They should have been tightly adherent since they were plated on polylysine coated surfaces. Observations were apparently in a plane a micron from the supporting surface					
C	67	Rat retinal pigmented cells (intracellular speeds in nondystrophic cells)	30 at 37	Fluo-3 AM	[134]
C	68	Rat megakaryocytes	35 at 23	Fura-2 AM	[135]
	69	Chick embryo osteoclasts	21 at 20 (? [136a])	Fura-2 AM	[136]
These were in a medium bearing 10% fetal calf serum when plated. So they should have been only loosely adherent to the supporting surface					
C	70	Human prostate cancer cell line	23 at 36	Fluo-3 AM	[137]
C	71	Human HeLa cell line	~16 at 24	Fluo-3 AM	[138]
Measured from author's Fig. 1a					
C	71a	Rat glial precursor cells	150 at 37	Fluo AM's	[138a]
C	72	Cell-free extract from pig skeletal muscle	45 at room T	Fluo-3 or -4	[139]
Ci	73	*Chara* cytoplasmic droplet	15 at 23	Rotation stops	[140]
From authors' Fig. 4					

'C' means a wave within a cell and such data are plotted in Fig. 1B. 'T' means a wave across a tissue or monolayer and such data plotted in Fig. 1C; 'i' means an inwards wave.
[a] Via letters from Drs Wier, Lederer and Cannell.
[b] From the authors' Fig. 8C.

In one very interesting–and perhaps key report (Table 1b's case #16 based upon [60]) speeds across ventriculocytes which are near the center of the conserved range were observed. In this paper (and also–if less clearly–in Table 1b's case #15dd–a low amplitude calcium wave was propagated *without any cell contraction.* Moreover (higher amplitude?) calcium waves–likewise through guinea pig ventriculocytes and from the same laboratory–were elicited by tripling the extracellular potassium level and thereby increasing intracellular calcium. These cells in a high potassium medium–unlike those in serum level potassium–seemed to undergo a contractile wave along with the calcium one. So these findings suggest that the anomalously high speeds across some ventriculocyte preparations are propagated by contraction.

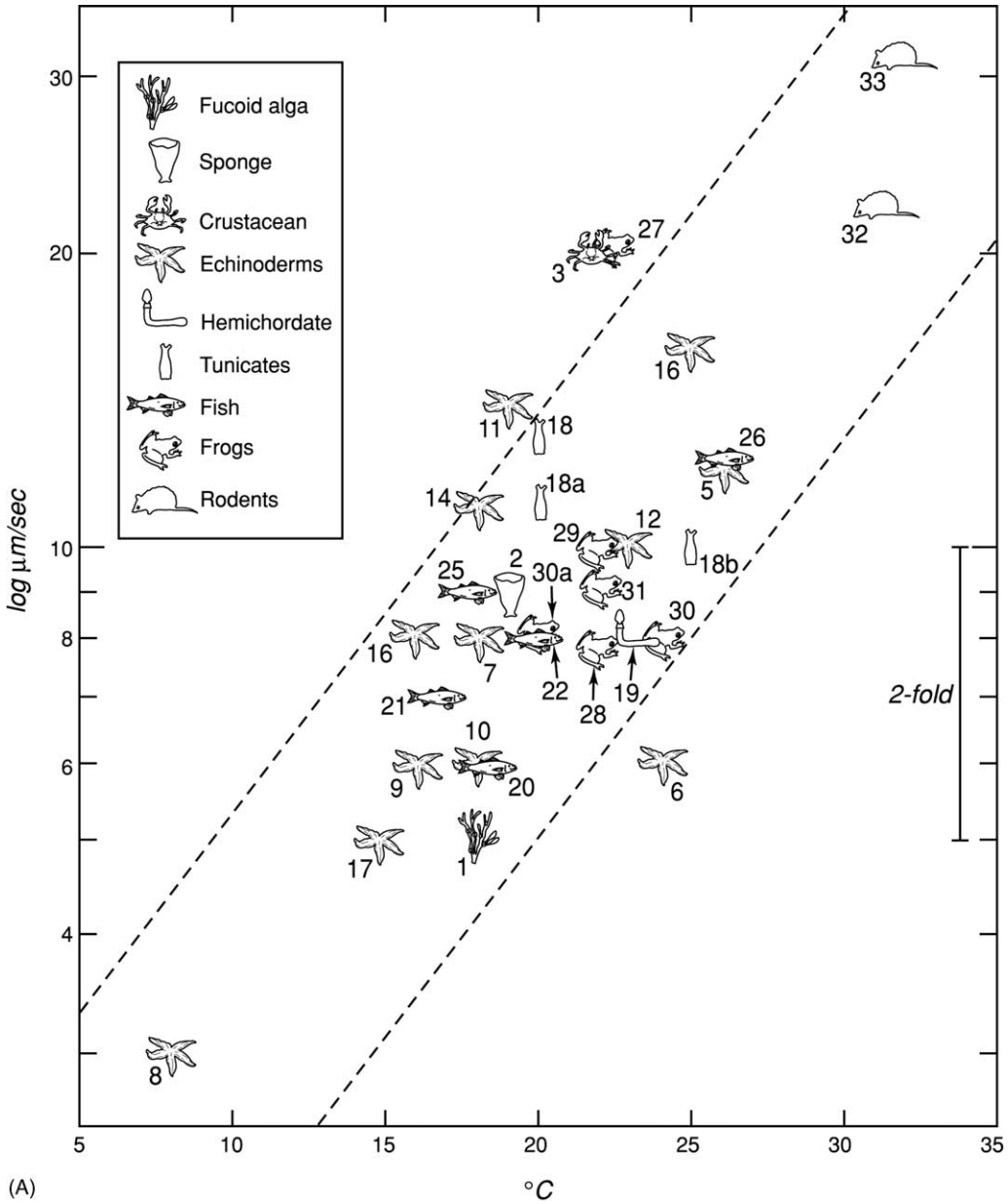

Fig. 1 (A) The speeds of egg activation or fertilization waves vs. temperature. Despite the fact that these data are from eggs which come from a fucoid alga and a sponge up to a shrimp and two rodents, most speeds lie within a 2–3-fold range at a given temperature. The speeds rise 2.7-fold per 10 °C over the available range of 8–32 °C. Extrapolation (not shown) predicts a speed of about 50 μm/s for the first fertilization wave across the human egg at body temperature. (B) The speeds of intracellular fast calcium waves within fully active cells vs. temperature. Although these data are from cells that go from droplets of algal cytoplasm (#73) up to the human brain (#26 and 26b), most speeds lie within a 3–4-fold range at a given temperature. The mean speed—of about 15 μm/s at 20 °C—is about twice that for the egg activation waves shown in (A). However, the collective Q_{10} is 2.7-fold per 10 °C as it is for activation waves. The waves in the upper outliers marked with a triangle may be propagated by CICE or calcium-induced calcium entry instead of CICR or calcium-induced calcium release. The value marked with a large open circle (#34) was from a wave entrapped within a retinal ring, may be the most accurate one ever measured and serves to compare these data with those through tissues shown in (C). (C) The speeds of fast calcium waves through tissues vs. temperature. The data come from very diverse systems including streak stage chicks (#7–7a), skate cerebella (#37), blowfly salivaries (#49), rat livers (#55) and the human brain during a migraine attack (#26–26b). Nevertheless, most of the data lie within a 2–3-fold range at a given temperature.

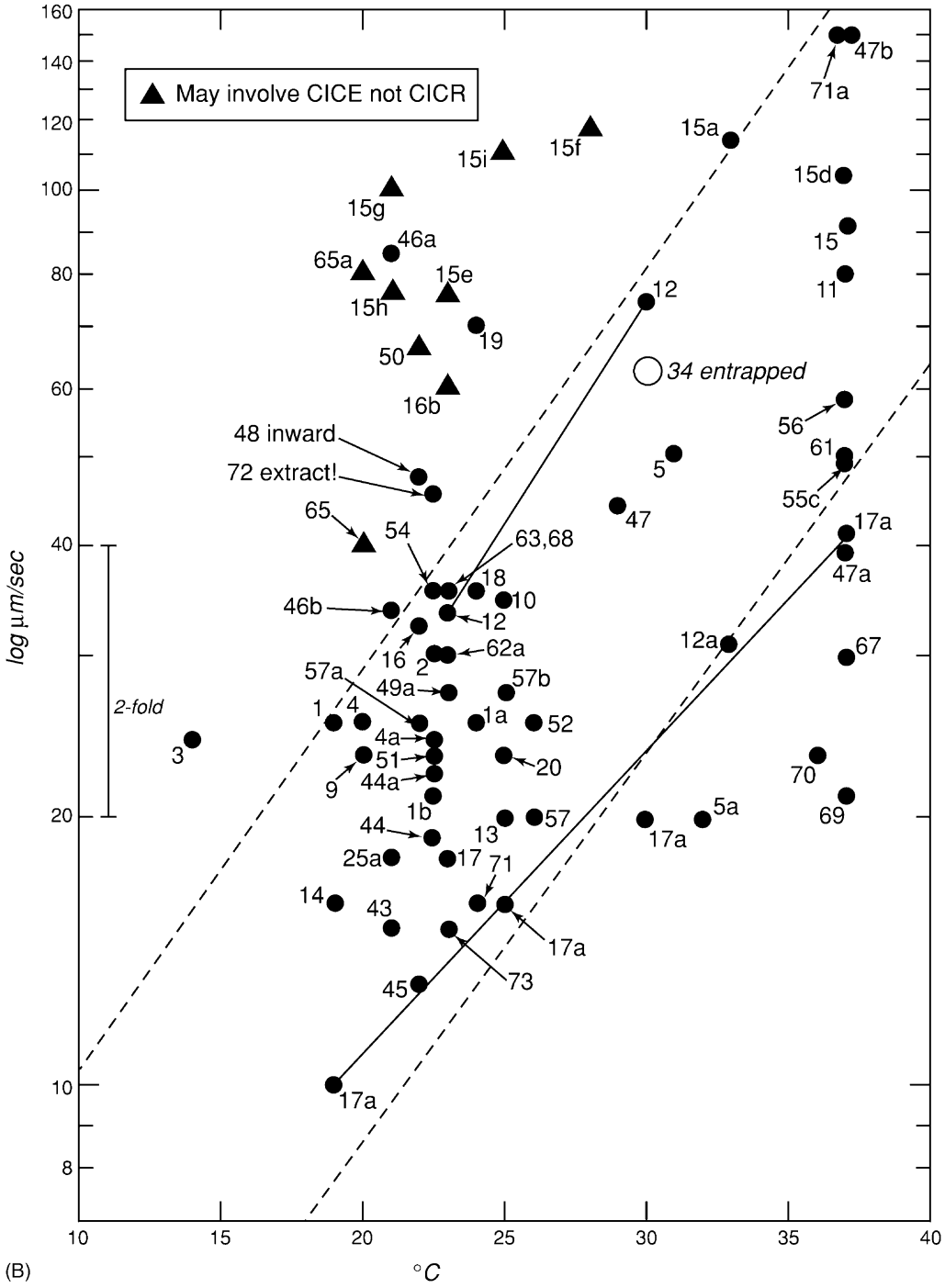

Fig. 1 (B)

The important class of slow calcium waves may also be propagated by contraction [4]; however, in the ultra-flat ventriculocytes, the obvious site of stretch sensitive channels would be in the plasma membrane rather than the ER. Local subsurface contraction could not stretch the nearby plasma membrane so as to open such channels if the cell were too loosely attached to the support so the suggested mechanism should only work for cells that are tightly attached to the support. With this in mind, I sought evidence favoring tight or loose attachment in

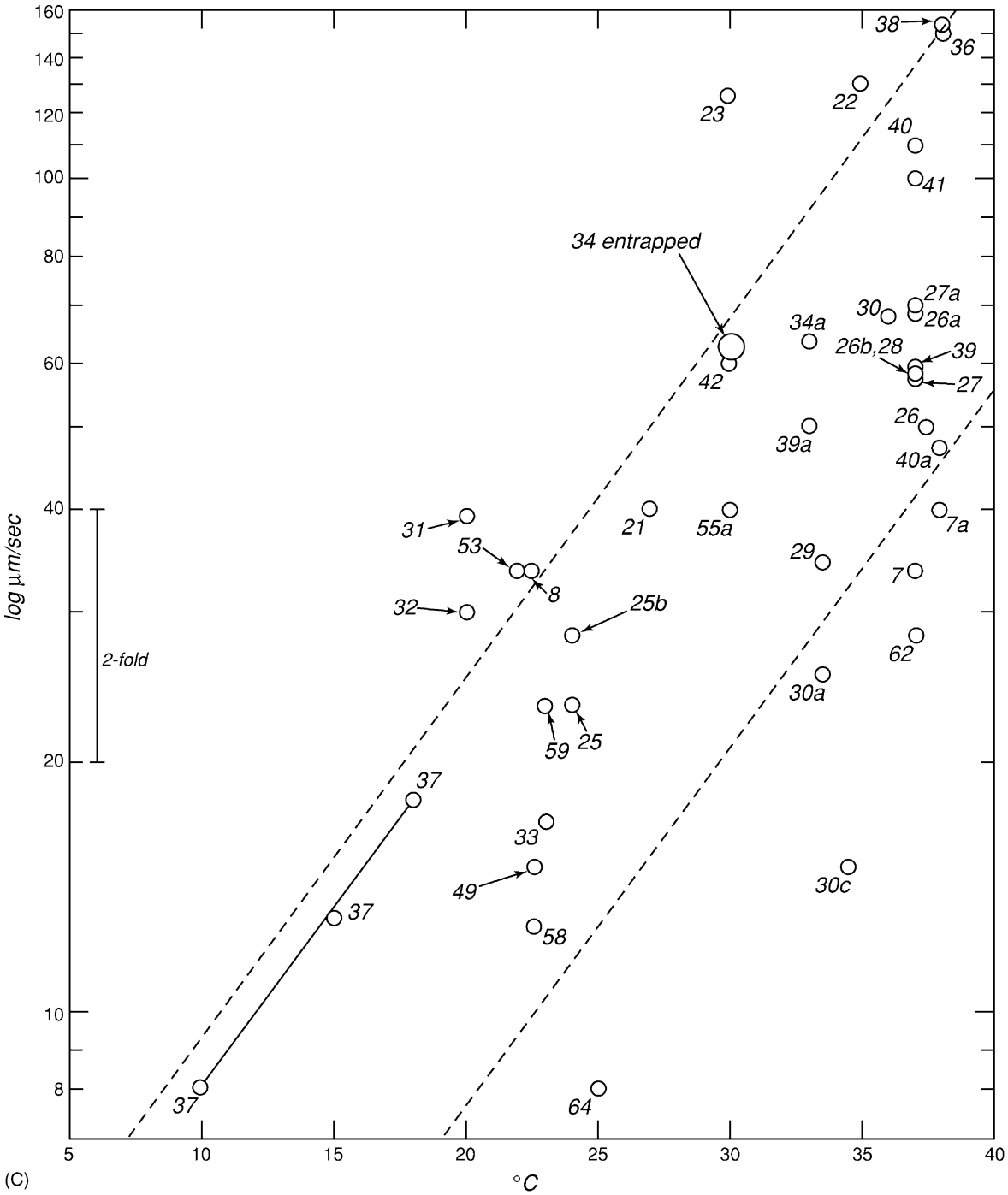

Fig. 1 (C)

the dozen or so reports of isolated ventriculocyte calcium wave speeds and have summarized this evidence in Table 1b. With one exception, the evidence does show the expected correlation between tight attachment and high speed. Moreover, in two other studies of isolated, flattened and adherent cells–that on goldfish keratocytes (case #50 via papers [111]) and on *Xenopus* pituitary melanotropes (case #65 via papers [132–134])–in both of these, calcium wave speeds were likewise 2–3-fold above the conserved range of fast wave speeds.

I would therefore propose that these high speeds–which are shown as dark triangles (▲) in Fig. 1B–are propagated

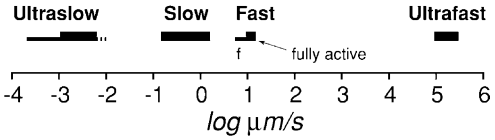

Fig. 2 Main classes of calcium waves based upon speed at room temperature. Note how narrow the ranges of fast waves are in this context; f, fertilization waves. Ultrafast means calcium propagated action potentials; slow, stretch propagated waves; ultraslow, various developmental ones. Modified from [3,4].

by what could be called calcium-induced calcium entry or perhaps better, *stretch propagated calcium entry* (SPCE). In it, local calcium entry would raise subsurface calcium. This would induce local contraction. This contraction would open nearby stretch-sensitive calcium channels in the plasmalemma so as to allow nearby calcium entry, and thus, continue the propagation cycle. It may be objected that these high speeds are not reduced by lowering calcium levels in the general medium. However, the proposed cycle would be propagated along the space *under* a plated ventriculocyte where calcium levels would be set by rapid local mechanisms and would be unaffected by calcium levels in the perfusion medium. Just before submitting this paper I read (or reread?) a very similar model that was put forward in 1995 by Wiltink et al. to explain their observations of fast waves through isolated osteoclasts. While I have developed an SPCE model to explain anomalously fast waves through certain preparations under highly artificial conditions, the SPCE model of Wiltink et al. has clear implications for natural bone development and remodeling.

In conclusion, this compilation indicates that all biological waves which move at about 10–30 μm/s at 20 °C (with temperature corrections shown in Fig. 1A–C) are propagated by the same fast wave mechanism. This is a reaction/diffusion one which is governed by the Luther equation in which the velocity, V is neither limited by the speed of the calcium-induced calcium release reaction (CICR), k nor by the diffusion constant of free calcium, D. Rather, velocity depends upon the square root of the product of k and D [2].

$$V \propto \sqrt{kD}$$

Finally, one may ask why evolution has conserved the mechanism of fast calcium waves. I would again suggest that it did so since they are propagated by a multiprotein, ER machine that is too complex and too vital to change after the ER's invention [4]. Moreover, I would again suggest that this complexity lies in a machine that drives two tandem waves of calcium that are just outside of and also within the ER and that both reinforce and constrain each other [144].

ACKNOWLEDGEMENTS

This work was supported by the National Library of Medicine via grant #1 G13 LM07022-01.

REFERENCES

1. Gilkey JC, Jaffe LF, Ridgway EB, Reynolds GT. A free calcium wave traverses the activating egg of the medaka, *Oryzias latipes*. *J Cell Biol* 1978; **76**: 448–466.
2. Jaffe LF. The path of calcium in cytosolic calcium oscillations: a unifying hypothesis. *Proc Natl Acad Sci USA* 1991; **88**: 9883–9887.
3. Jaffe LF. Organization of early development by calcium patterns. *Bioessays* 1999; **21**: 657–667.
4. Jaffe LF, Créton R. On the conservation of calcium wave speeds. *Cell Calcium* 1998; **24**: 1–8.
5. Knapp E. Entwicklungsphysiologie Untersuchungen an Fucaceen-Eiern. *Planta* 1931; **14**: 731–751.
6. Kume M. Note on the early development of *Tethya serica* Lebwohl, a tetraxonian sponge. *Natl Sci Rep Ochanomizu Univ* 1952; **3**: 63–67.
7. Lindsay LL, Hertzler PL, Clark WH. Extracellular Mg^{2+} induces an intracellular Ca^{2+} wave during oocyte activation in the marine shrimp *Sicyonis ingentis*. *Dev Biol* 1992; **152**: 94–102.
8. Moser F. Studies on a cortical layer response to stimulating agents in the *Arbacia* egg. *J Exp Zool* 1939; **80**: 423–472.
9. Dan JC, Dan K. Early development of *Comanthus japonica*. *Jpn J Zool* 1941; **9**: 565–574.
10. Kacser H. The cortical changes on fertilization of the sea urchin egg. *J Exp Biol* 1955; **32**: 451–467.
11. Ginzburg AS. The mechanism of blocking of polyspermia in echinoderms. *Dokl Akad Nauk SSSR* 1964; **152**: 1232–1235.
12. Paul M, Epel D. Fertilization–associated light-scattering changes in eggs of the sea urchin *Strongylocentrotus purpuratus*. *Exp Cell Res* 1971; **65**: 281–288.
13. Eisen A, Reynolds GT. Calcium transients during early development in single starfish (*Asterias forbesi*) oocytes. *J Cell Biol* 1984; **99**: 1878–1882.
14. Eisen A, Kiehart DP, Wieland SJ, Reynolds GT. Temporal sequence and spatial distribution of early events of fertilization in single sea urchin eggs. *J Cell Biol* 1984; **99**: 1647–1654.
15. Yoshimoto Y, Iwamatsu T, Hirano K-I, Hiramoto Y. The wave pattern of free calcium release upon fertilization in medaka and sand dollar eggs. *Dev Growth Differ* 1986; **28**: 583–596.
16. Swann K, Whitaker M. The part played by inositol trisphosphate and calcium in the propagation of the fertilization wave in sea urchin eggs. *J Cell Biol* 1986; **103**: 2333–2342.
17. Hafner M, Petzelt C, Nobiling R, Pawley JB, Kramp D, Schatten G. Wave of free calcium at fertilization in the sea urchin egg visualized with fura-2. *Cell Motil Cytoskeleton* 1988; **9**: 271–277.
18. Hamaguchi Y, Hamaguchi MS. Simultaneous investigation of intracellular Ca^{2+} increase and morphological events upon fertilization in the sand dollar egg. *Cell Struct Funct* 1990; **15**: 159–162.
19. Stricker SA. Repetitive calcium waves induced by fertilization in the nemertian worm *Cerebratulus lacteus*. *Dev Biol* 1996; **176**: 243–263.

20. Speksnijder JE, Sardet C, Jaffe LF. The activation wave of calcium in the ascidian egg and its role in ooplasmic segregation. *J Cell Biol* 1990; **110**: 1589–1598.
21. Yoshida M, Sensui N, Inoue T, Morisawa M, Mikoshiba K. Role of two series of Ca^{2+} oscillations in activation of ascidian eggs. *Dev Biol* 1998; **203**: 122–133.
22. Wilding M, Marino M, Monfrecola V, Dale B. Meiosis-associated calcium waves in ascidian oocytes are correlated with the position of the male centrosome. *Zygote* 2000; **8**: 285–293.
23. Colwin LH, Colwin AL. Fertilization changes in the membranes and cortical granular layer of the egg of *Saccoglossus lowalevskii* (Enteropneusta). *J Morphol* 1954; **95**: 1–46.
24. Yamamoto T. Physiology of fertilization and activation of the egg of the sand lamprey. *Zool Mag (Tokyo)* 1947; **57**: 164–166.
25. Thomopoulos A. Sur l'oeuf de *Perca fluviatilis* L. *Bull Soc Zool Fr* 1953a; **78**: 106–114.
26. Thomopoulus A. Sur l'oeuf de l'epinoche *Gasterosteus aculeatus* L. *Bull Soc Zool Fr* 1953b; **78**: 142–149.
27. Kusa M. Studies on cortical alveoli in some teleostean eggs. *Embryologia* 1956; **3**: 141–153.
28. Yoshimoto Y, Iwamatsu T, Hirano K-I, Hiramoto Y. The wave pattern of free calcium release upon fertilization in medaka and sand dollar eggs. *Dev Growth Differ* 1986; **28**: 583–596.
29. Goldenberg M, Elinson RP. Animal/vegetal differences in cortical granule exocytosis during activation of the frog egg. *Dev Growth Differ* 1980; **22**: 345–356.
30. Kubota HY, Yoshimoto Y, Yoneda M, Hiramoto Y. Free activation wave upon activation in Xenopus eggs. *Dev Biol* 1987; **119**: 129–136.
31. Busa W, Nuccitelli R. An elevated free cytosolic Ca^{2+} wave follows fertilization in eggs of the frog, *Xenopus laevis*. *J Cell Biol* 1985; **100**: 1325–1329.
32. Galione A, McDougall A, Busa WB, Willmott N, Gillott I, Whitaker M. Redundant mechanisms of calcium-induced calcium release underlie calcium waves during fertilization of sea urchin eggs. *Science* 1993; **261**: 348–352.
33. Yao Y, Choi J, Parker I. Quantal puffs of intracellular Ca^{2+} evoked by inositol trisphosphate in *Xenopus* oocytes. *J Physiol* 1995; **482.3**: 533–553.
34. Fontanilla RA, Nuccitelli RA. Characterization of the sperm-induced calcium wave in *Xenopus* eggs using confocal microscopy. *Biophys J* 1998; **75**: 2087–2097.
35. Miyazaki S-I, Hashimoto N, Yoshimoto Y, Kishimoto T, Igusa Y, Hiramoto Y. Temporal and spatial dynamics of the periodic increase in intracellular free calcium at fertilization of golden hamster eggs. *Dev Biol* 1986; **118**: 259–267.
36. Deguchi R, Shirakawa H, Oda S, Mohri T, Miyazaki S. Spatiotemporal analysis of Ca^{2+} waves in relation to the sperm entry site and animal–vegetal axis during Ca^{2+} oscillations in fertilized mouse eggs. *Dev Biol* 2000; **218**: 299–313.
37. DeLisle S, Welsh MJ. Inositol trisphosphate is required for the propagation of calcium waves in *Xenopus* oocytes. *J Biol Chem* 1992; **267**: 7963–7966.
38. Girard S, Clapham D. Acceleration of intracellular calcium waves in *Xenopus* oocytes by calcium influx. *Science* 1993; **260**: 229–232.
39. Camacho P, Leichleiter JD. Increased frequency of calcium waves in *Xenopus laevis* oocytes that express a calcium-ATPase. *Science* 1993; **260**: 226–229.
40. Callameras N, Marchant JS, Sun X-P, Parker I. Activation and co-ordination of $InsP_3$-mediated elementary Ca^{2+} events during global Ca^{2+} signals in *Xenopus* oocytes. *J Physiol* 1998; **509.1**: 81–91.
41. Jouaville LS, Ichas F, Holmuhamedov L, Camacho P, Leichleiter J. Synchronization of calcium waves by mitochondrial substrates in *Xenopus laevis* oocytes. *Nature* 1995; **377**: 438–441.
42. Eckberg WR, Miller AL. Propagated and nonpropagated calcium transients during egg activation in the annelid *Chaetopterus*. *Dev Biol* 1995; **172**: 654–664.
43. Wilding M, Marino M, Monfrecola V, Dale B. Meiosis-associated calcium waves in ascidian oocytes are correlated with the position of the male centrosome. *Zygote* 2000; **8**: 285–293.
44. Tesarik J, Testart J. Treatment of sperm-injected human oocytes with Ca^{2+} ionophore supports the development of Ca^{2+} oscillations. *Biol Reprod* 1994; **51**: 385–391.
45. Stern C, Goodwin B. Waves and periodic events during primitive streak formation in the chick. *J Embryol Exp Morphol* 1977; **41**: 15–22.
46. Drews U, Mengis W. Contraction wave in the chick blastoderm induced by muscarinic stimulation. *Anat Embryol* 1990; **182**: 447–454.
47. Barber B, da Cruz MJB, DeLeon J, Fluck RA, Hasenfeld MP, Unis LA. Pacemaker region in a rhythmically contracting embryonic epithelium, the enveloping layer of *Oryzias latipes*, a teleost. *J Exp Zool* 1987; **242**: 35–42.
48. Reuben JP, Brandt PW, Grundfest H. Regulation of myoplasmic calcium concentration in intact crayfish muscle fibers. *J Mechanochem Cell Motil* 1974; **2**: 269–285.
49. Chawla S, Skepper JN, Hockaday AR, Huang CL-H. Calcium waves induced by hypertonic solutions in intact frog skeletal muscle fibres. *J Physiol* 2001; **536.2**: 351–359.
50. Minimakawa T, Cody SH, Williams DA. In situ visualization of spontaneous calcium waves within perfused whole rat heart by confocal by confocal imaging. *Am J Physiol* 1997; **272**: H236–H243.
51. Kort AA, Capogrossi MC, Lakatta EG. Frequency, amplitude, and propagation velocity of spontaneous Ca^{2+}-dependent contractile waves in intact adult rat cardiac muscle and isolated myocytes. *Circ Res* 1985; **57**: 844–855.
52. Wier WG, ter Keurs HEDJ, Marban E, Gao WD, Balke CW. Ca^{2+} 'sparks' and waves in intact ventricular muscle resolved by confocal imaging. *Circ Res* 1997; **81**: 462–469.
53. Ruehlmann DOD, Lee C-H, Poburko Dvan Breeman C. Asynchronous Ca^{2+} waves in intact venous smooth muscle. *Circ Res* 2000; **86**: e72–e79.
54. Blatter LA, Wier WG. Agonist-induced $[Ca^{2+}]_i$ waves and Ca^{2+}-induced Ca^{2+} release in mammalian vascular smooth muscle cells. *Am J Physiol* 1992; **263**: H576–H886.
55. Capogrossi MC, Lakatta EG. Frequency moculation and synchronization of spontaneous oscillations in cardiac cells. *Am J Physiol* 1985; **248**: H412–H418.
56. Wier WG, Cannell MB, Berlin JR, Marban E, Lederer WJ. Cellular and subcellular heterogeneity of $[Ca^{2+}]_i$ in single heart cells revealed by fura-2. *Science* 1987; **235**: 325–328.
57. Grouselle M, Stuyvers B, Bonoron-Adele S, Besse P, Georgescauld D. Digital-imaging microscopy analysis of calcium release from sarcoplasmic reticulum in single rat cardiac myocytes. *Pfluegers Arch Eur Physiol* 1991; **418**: 109–119;
(a) Engel J, Fechner M, Sowerby AJ, Finch SAE, Stier A. Anisotropic propagation of Ca^{2+} waves in isolated cardiomyocytes. *Biophys J* 1994; **66**: 1756–1762.

58. Engel J, Sowerby AJ, Finch SAE, Fechner M, Stier A. Temperature dependence of Ca^{2+} wave properties in cardiomyocytes: implications for the mechanism of autocatalytic Ca^{2+} release. *Biophys J* 1995; **68**: 40–45.
59. López JR, Jovanovic A, Terzic A. Spontaneous calcium waves without contraction in cardiac myocytes. *Biochem Biophys Res Commun* 1995; **214**: 781–787.
60. Ishida N, Urayama T, Inoue K-I, Komaru T, Takishima T. Propagation and collision characteristics of calcium waves in rat myocytes. *Am J Physiol* 1990; **259**: H940–H950.
61. Williams DA, Delbridge LM, Cody SH, Harris PJ, Morgan TO. Spontaneous and propagated calcium release in isolated cardiac myocytes viewed by confocal microscopy. *Am J Physiol* 1992; **262**: C731–C742.
62. Chen W, Steenbergen C, Levy LA, Vanc J, London RE, Murphy E. Measurement of free Ca^{2+} in sarcoplasmic reticulum in perfused rabbit heart loaded with 1,2-bis(2-amino-5,6-difluorophenoxy)ethane-*N,N,N′N′*-tetracetic acid by ^{19}F NMR. *J Biol Chem* 1996; **271**: 7398–7403.
63. López JR, Jovanovic A, Terzic A. A K_{ATP} channel opener protects cardiomyocytes from Ca^{2+} waves: a laser confocal microscopy study. *Am J Physiol* 1996; **270**: H1384–H1389.
64. Wussling MHP, Salz H. Nonlinear propagation of spherical calcium waves in rat cardiac myocytes. *Biophys J* 1996; **70**: 1144–1153.
65. Young RC, Hession RO. Paracrine and intracellular signalling mechanisms of calcium waves in cultured human uterine myocytes. *Obstet Gynecol* 1997; **90**: 928–932.
66. Young RC, Zhang P. The mechanism of propagation of intracellular calcium waves in cultured human uterine myocytes. *Am J Obstet Gynecol* 2001; **184**: 1228–1234.
67. Flucher BE, Andrews SB. Characterization of spontaneous and action potential-induced calcium transients in developing myotubes in vitro. *Cell Motil Cytoskeleton* 1993; **25**: 143–157.
68. Mayer EA, Kodner A, Ping Sun X, Wilkes J, Scott D, Sachs G. Spatial and temporal patterns of intracellular calcium in colonic smooth muscle. *J Membr Biol* 1992; **125**: 107–118.
69. Burgi P-Y, Grzywacz NM. Model for the pharmacological basis of spontaneous activity in developing retinas. *J Neurosci* 1994; **14**: 7426–7439.
70. Catsicas M, Bonness V, Becker D, Mobbs P. Spontaneous Ca^{2+} transients and their transmission in the developing chick retina. *Curr Biol* 1998; **8**: 283–286.
71. Bansai A, Singe JH, Hwang BJ, Xu W, Beaudet A, Feller MB. Mice lacking specific nicotinic acetylcholine receptor subunits exhibit dramatically altered spontaneous activity patterns and reveal a limited role for retinal waves in forming ON and OFF circuits in the inner retina. *J Neurosci* 2000; **20**: 7672–7681.
72. Meister M, Wong ROL, Baylor DA, Shatz CJ. Synchronous bursts of action potentials in ganglion cells of the developing mammalian retina. *Science* 1991; **252**: 939–943.
73. Feller MB, Wellis DP, Stellwagen D, Werblin FS, Shatz CJ. Requirement for cholinergic synaptic transmission in the propagation of spontaneous retinal waves. *Science* 1996; **272**: 1182–1187.
74. Stellwagen D, Shatz CJ, Feller MB. Dynamics of retinal waves are controlled by cyclic AMP. *Neuron* 1999; **24**: 673–685.
75. Newman EA, Zahs KR. Calcium waves in retinal glial cells. *Science* 1997; **275**: 844–847.
76. Li Y, Holtzclaw LA, Russell JT. Müller cell Ca^{2+} waves evoked by purinergic receptor agonists in slices of rat retina. *J Neurophysiol* 2001; **85**: 986–994.
77. Newman EA. Propagation of intercellular calcium waves in retinal astrocytes and Muller cells. *J Neurosci* 2001; **21**: 2215–2223.
78. Lashley KS. Patterns of cerebral integration indicated by the scotomas of migraine. *Arch Neurol Psychiatr* 1941; **46**: 331–339.
79. Cao Y, Welch KMA, Aurora S, Vikingstad EM. Functional MRI-BOLD of visually triggered headache in patients with migraine. *Arch Neurol* 1999; **56**: 548–554.
80. Hadjikhani N, Sanchez del Rio M, Wu O et al. Mechanisms of migraine aura revealed by functional MRI in human visual cortex. *Proc Natl Acad Sci USA* 2001; **98**: 4687–4692.
81. Hasegawa Y, Latour LL, Formato JE, Sotak CH, Fisher M. Spreading waves of a reduced diffusion coefficient of water in normal and ischemic rat brain. *J Cereb Blood Flow Metab* 1995; **15**: 179–187.
82. Beaulieu C, Busch E, de Crespigny A, Moseley ME. Spreading waves of transient and prolonged decreases in water diffusion after subarachnoid hemorrhage in rats. *Magn Reson Med* 2000; **44**: 110–116.
83. Bockhorst KHJ, Smith JM, Smith MI et al. A quantitative analysis of cortical spreading depression events in the feline brain characterized with diffusion-weighted MRI. *J Magn Res* 2000; **12**: 722–733.
84. Basarsky TA, Duffy SN, Andrew RD, MacVicar BA. Imaging spreading depression and associated intracellular calcium waves in brain slices. *J Neurosci* 1998; **18**: 7189–7199.
85. Kunkler PE, Kraig RP. Calcium waves precede electrophysiological changes of spreading depression in hippocampal organ cultures. *J Neurosci* 1998; **18**: 3416–3425.
86. Aitken PG, Tombaugh GC, Turner DA, Somjen GG. Similar propagation of SD and hypoxic SD-like depolarization in rat hippocampus recorded optically and electrically. *J Neurophysiol* 1998; **80**: 1514–1521.
87. Schadé JP, Collewijn H. Neurological studies on cephalopods. I. Spreading depression and impedance changes in the retina. *Neth J Sea Res* 1964; **2**: 123–144.
88. Gouras P. Spreading depression of activity in amphibian retina. *Am J Physiol* 1958; **195**: 28–32.
89. Martins-Ferreira H, Oliveira-Castro G, Struchner CJ, Rodrigues PS. Circling spreading depression in isolated chick retina. *J Neurophysiol* 1974; **37**: 773–784.
90. Gorelova NA, Bures J. Spiral waves of spreading depression in the isolated chicken retina. *J Neurobiol* 1983; **14**: 353–363.
91. Kraig RP, Nicholson C. Extracellular ionic variations during spreading depression. *Neuroscience* 1978; **3**: 1045–1059.
92. Young W. Spreading depression in elasmobranch cerebellum. *Brain Res* 1980; **199**: 113–126.
93. Tobiasz C, Nicholson C. Tetrodotoxin resistant propagation and extracellular sodium changes during spreading depression in rat cerebellum. *Brain Res* 1982; **241**: 329–333.
94. Schadé JP. Maturational aspects of EEG and of spreading depression in rabbit. *J Neurophysiol* 1959; **22**: 245–257.
95. Boone K, Lewis AM, Holder DS. Imaging of cortical spreading depression by EIT: implications for localization of epileptic foci. *Physiol Meas* 1994; **15**: A189–A198.
96. Albe-Fessard D, Sanderson P, Condes-Lara M, Delandsheer E, Giuffrida R, Cesaro P. Utilisation de la depression envahissante de Leão pur l'etude de relations entre structures centrales. *An Acad Bras Cienc* 1984; **56**: 371–383.
97. Lauritzen M, Fabricius M. Real time laser-Doppler perfusion imaging of cortical spreading depression in rat neocortex. *Neuroreport* 1995; **6**: 1271–1273.

98. Herreras O, Somjen GG. Propagation of spreading depression among dendrites and somata of the same cell population. *Brain Res* 1993; **610**: 276–282.
99. Federico P, MacVicar BA. Imaging the induction and spread of seizure activity in the isolated brain of the guinea pig. *J Neurophysiol* 1996; **76**: 3471–3492;
    (a) Federico P, Borg SG, Salkaukus AG, MacVicar BA. Mapping patterns of neuronal activity and seizure propagation by imaging intrinsic optical signals in the isolated whole brain of the guinea-pig. *Neuroscience* 1994; **58**: 461–480.
100. Dani JW, Chernjavsky A, Smith SJ. Neuronal activity triggers Ca^{2+} waves in hippocampal astrocyte network. *Neuron* 1992; **8**: 429–440.
101. Cornell-Bell AH, Finkbeiner SM, Cooper SM, Smith SJ. Glutamate induces calcium waves in cultured astrocytes. *Science* 1990; **247**: 470–473.
102. Finkbeiner S. Calcium waves in astrocytes–filling in the gaps. *Neuron* 1992; **8**: 1101–1108.
103. Yagodin SV, Holtzclaw L, Sheppard CA, Russell JT. Nonlinear propagation of agonist-induced cytoplasmic calcium waves in single astrocytes. *J Neurobiol* 1994; **25**: 265–280.
104. Reber BFX, Schindelholz B. Detection of a trigger zone of bradykinin-induced fast calcium waves in PC12 neurites. *Pflugers Arch* 1996; **432**: 893–903.
105. Wang SS, Thompson SH. Local positive feedback by calcium in the propagation of intracellular calcium waves. *Biophys J* 1995; **69**: 1683–1697.
106. Fink CC, Slepchenko B, Moraru II, Watras J, Schaff JC, Loew LM. An image-based model of calcium waves in differentiated neuroblastoma cells. *Biophys J* 2000; **79**: 163–183.
107. Hua S-Y, Liu C, Lu F-M, Nohmi M, Kuba K. Modes of propagation of Ca^{2+}-induced Ca^{2+} release in bullfrog sympathetic ganglion cells. *Cell Calcium* 2000; **27**: 195–204.
108. Nohmi M, Hua S-Y, Liu C, Kuba K. Ryanodine- and thapsigargin-Ca^{2+}-induced Ca^{2+} release is primed by lowering external Ca^{2+} in rabbit autonomic neurons. *Pflugers Arch Eur J Physiol* 2000; **440**: 588–599.
109. Zimmerman B, Walz B. The mechanism mediating regenerative intercellular Ca^{2+} waves in the blowfly salivary gland. *EMBO J* 1999; **18**: 3222–3231.
110. Zimmermann B. Subcellular organization of agonist-evoked Ca^{2+} waves in the blowfly salivary gland. *Cell Calcium* 2000; **27**: 297–307.
111. Brust-Mascher I, Webb WW. Calcium waves induced by large voltage pulses in fish keratocytes. *Biophys J* 1998; **75**: 1669–1678.
112. Hirata K, Nathanson MH, Burgstahler AD, Okazaki K, Mattei E, Sear ML. Relationship between inositol 1,4,5-trisphosphate receptor isoforms and subcellular Ca^{2+} signaling patterns in nonpigmented ciliary epithelia. *Invest Ophthamol Vis Sci* 1999; **40**: 2046–2053.
113. Toescu EC, Lawrie AM, Petersen OH, Gallacher DV. Spatial and temporal distribution of agonist-evoked cytoplasmic Ca^{2+} signals in exocrine acinar cells analysed by digital image microscopy. *EMBO J* 1992; **11**: 1623–1629.
114. Churchill GC, Louis CF. Roles of Ca^{2+}, inositol trisphosphate and cyclic ADP-ribose in mediating intercellular Ca^{2+} signaling in sheep lens cells. *J Cell Sci* 1998; **111**: 1217–1225.
115. Nathanson MH, O'Neill AF, Burgstahler AD. Primitive organization of cytosolic Ca^{2+} signals in hepatocytes from the little skate *Raja erinacea*. *J Exp Biol* 1999; **202**: 3049–3056.
116. Nathanson MH, Burgstahler AD, Mennone A, Fallon MB, Gonzalez CB, Saez JC. Ca^{2+} waves are organized among hepatocytes in the intact organ. *Am J Physiol* 1995; **269**: G167–G171.
117. Robb-Gaspers LD, Thomas AP. Coordination of Ca^{2+} signaling by intercellular propagation of Ca^{2+} waves in the intact liver. *J Biol Chem* 1995; **270**: 8102–8107.
118. Nathanson MH, Burgstahler AD, Fallon MB. Multistep mechanism of polarized Ca^{2+} wave patterns in hepatocytes. *Am J Physiol* 1994; **267**: G338–G349.
119. Fox JL, Burgstahler AD, Nathanson MH. Mechanism of long-range Ca^{2+} signalling in the nucleus of isolated rat hepatocytes. *Biochem J* 1997; **326**: 491–495.
120. Nathanson MH, Padfield PJ, O'Sullivan AJ, Burgstahler AD, Jamieson JD. Mechanism of Ca^{2+} wave propagation in pancreatic acinar cells. *J Biol Chem* 1992; **267**: 18118–18121.
121. Toescu EC, Lawrie AM, Petersen OH, Gallacher DV. Spatial and temporal distribution of agonist-evoked cytoplasmic Ca^{2+} signals in exocrine acinar cells analysed by digital image microscopy. *EMBO J* 1992; **11**: 1623–1629.
122. Gonzalez A, Pfeiffer F, Schmid A, Schulz I. Effect of intracellular pH on acetylcholine-induced Ca^{2+} waves in mouse pancreatic acinar cells. *Am J Physiol* 1998; **275**: C810–C817.
123. Pfeiffer F, Sternfeld L, Schmid A, Schulz I. Control of Ca^{2+} wave propagation in mouse pancreatic acinar cells. *Am J Physiol* 1998; **274**: C663–C672.
124. Hinman LE, Beilman GJ, Groehler KE, Sammak PJ. Wound-induced calcium waves in alveolar type II cells. *Am J Physiol* 1997; **273**: L1242–L1248.
125. Sanderson MJ, Charles AC, Dirksen ER. Mechanical stimulation and intercellular communication increases intracellular Ca^{2+} in epithelial cells. *Cell Regul* 1990; **1**: 585–596.
126. Tsunoda Y. Oscillatory Ca^{2+} signaling and its cellular function. *Cell Calcium* 1991; **3**: 3–17.
127. Jacob R. Imaging cytoplasmic free calcium in histamine stimulated endothelial cells and in fMet–Leu–Phe stimulated neutrophils. *Cell Calcium* 1990; **11**: 241–249.
128. Sammak PJ, Hinman LE, Tran PO, Sjaastad MD, Machen TE. How do injured cells communicate with the surviving cell monolayer? *J Cell Sci* 1997; **110**: 465–475.
129. Isshiki M, Ando J, Korenaga R et al. Endothelial Ca^{2+} waves preferentially originate at specific loci in caveolin-rich cell edges. *Proc Natl Acad Sci USA* 1998; **95**: 5009–5014.
130. Katagiri S, Takamatsu T, Minamikawa T, Fujita S. Secretogogue-induced calcium wave shows higher and prolonged transients of nuclear calcium concentration in mast cells. *FEBS Lett* 1993; **334**: 343–346.
131. Osipchuk Y, Cahalan M. Cell-to-cell spread of calcium signals mediated by ATP receptors in mast cells. *Nature* 1992; **359**: 241–244.
132. Scheenen WJJM, Jenks BG, van Dinter RJAM, Roubos EW. Spatial and temporal aspects of Ca^{2+} oscillations in *Xenopus laevis* melanotrope cells. *Cell Calcium* 1996; **19**: 219–227.
133. Koopman WJH, Hink MA, Visser JWG, Roubos EW, Jenks BG. Evidence that Ca^{2+}-waves in *Xenopus* melanotropes depend on calcium-induced calcium release. *Cell Calcium* 1999; **26**: 59–67.
134. Stahlmans P, Himpens B. Properties of intra- and intercellular Ca^{2+}-wave propagation elicited by mechanical stimulation in cultured RPE cells. *Cell Calcium* 1999; **25**: 391–399.

135. Tertyshnikova S, Fein A. $[Ca^{2+}]_i$ oscillations and $[Ca^{2+}]_i$ waves in rat megakaryocytes. *Cell Calcium* 1997; **21**: 331–344.
136. Wiltink A, Neiweide PJ, Scheenen WJJM, Ypey DL, Van Duijn B. Cell membrane stretch in osteoclasts triggers a self-reinforcing Ca^{2+} entry pathway. *Pflugers Arch Eur Physiol* 1995; **429**: 663–671;
(a) Wiltink A et al. Heterogeneity of calcium responses to parathyroid hormone and thrombin in primary osteoblast-like cells and UMR106-01 cells. *Cell Calcium* 1993; **14**: 591–600.
137. Perret S, Cantereau A, Audin J, Dufy B, Georgescauld D. Interplay between Ca^{2+} release and Ca^{2+} influx underlies localized hyperpolarization-induced $[Ca^{2+}]_i$ waves in prostatic cells. *Cell Calcium* 1999; **25**: 297–311.
138. Bootman M, Niggli E, Berrridge M, Lipp P. Imaging the hierarchical Ca^{2+} signalling system in HeLa cells. *J Physiol* 1997; **499**: 307–314;
(a) Haak LL, Grimaldi M, Smaili SS, Russell JT. Mitochondria regulate Ca^{2+} wave initiation and inositol trisphosphate signal transduction in oligodendrocyte progenitors. *J Neurochem* 2002; **80**: 405–415.
139. Wussling MHP, Krannich K, Drygalla V, Podsaisky H. Calcium waves in agarose gel with cell organelles: implications of the velocity curvature relationship. *Biophys J* 2001; **80**: 2658–2666.
140. Hayama T, Shimmen T, Tazawa M. Participation of Ca^{2+} in cessation of cytoplamic streaming induced by membrane excitation in *Characeae* internodal cells. *Protoplasma* 1979; **99**: 305–321.
141. Stephano JL, Gould MC. The intracellular calcium increase at fertilization in *Urechis caupo* oocytes: activation without waves. *Dev Biol* 1997; **191**: 53–68.
142. Lipp P, Niggli E. Microscopic spiral waves reveal positive feedback in subcellular calcium signaling. *Biophys J* 1993; **65**: 2272–2276.
143. Engel J, Fechner M, Sowerby AJ, Finch SAE, Stier A. Anisotropic propagation of Ca^{2+} waves in isolated cardiomyocytes. *Biophys J* 1994; **66**: 1756–1762.
144. Jaffe LF. Classes and mechanisms of calcium waves. *Cell Calcium* 1993; **14**: 736–745.